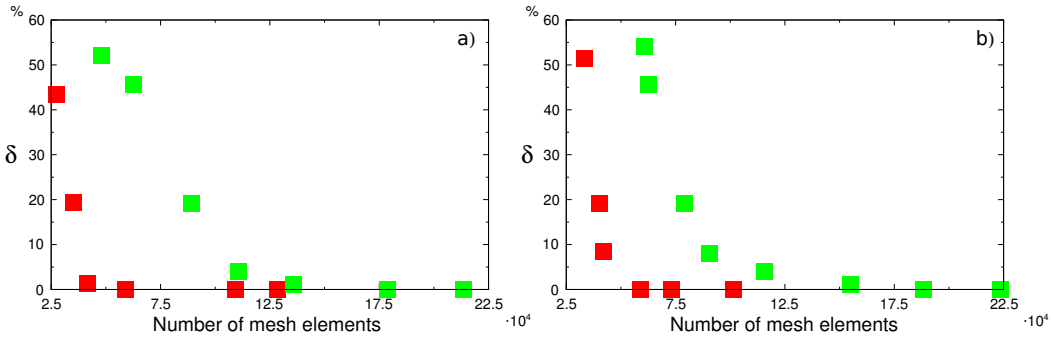

Supplementary Figure 1: Panel a) Relative error δ of the absorption cross section $\sigma_{\rm abs}$ versus number of mesh element for Na cylidrical nanowires for two radii: radius $R = 2\,$nm (red squares) and radius $R = 20\,$nm (green squares). Panel b) Same as Panel a), now for Ag nanowires.

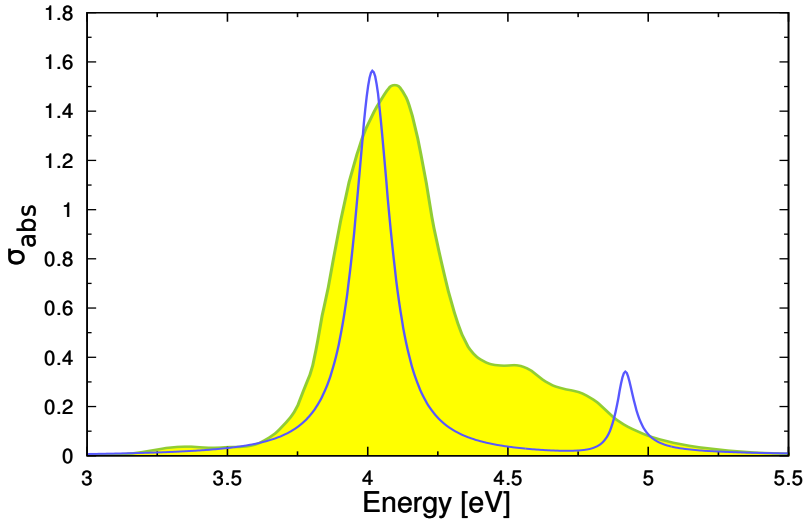

Supplementary Figure 2: Absorption spectra for a Na nanowire with radius $R = 2\,$nm obtained with the SC-HDM (blue line) and with the TD-DFT Octopus package by Stella *et al.* in ref 10 (green line with yellow filling).

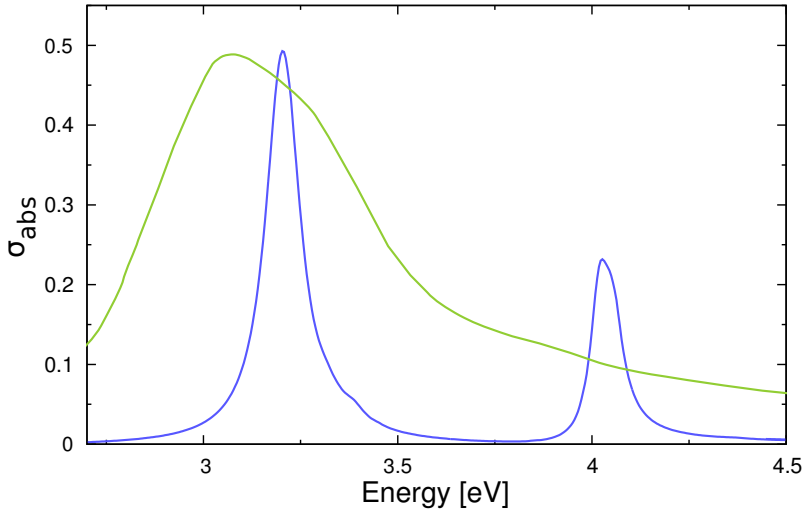

Supplementary Figure 3: Absorption spectrum for the Na_{331} cluster (effective radius $R_C = 1.439\,\text{nm}$) obtained by Li *et al.* [11] (green line) compared with the absorption nanowire with radius $R = 1.5\,\text{nm}$ obtained with the SC-HDM (blue line). The TD-LDA absorption spectrum is expressed in arbitrary units, since it is given in terms of dipole oscillator strengths in ref. 11.

Supplementary Note 1

The general formulation of the hydrodynamic model [1] is represented by the following Hamiltonian functional [2, 3]:

$$H[n(\mathbf{r},t),\mathbf{p}(\mathbf{r},t)] = G[n(\mathbf{r},t)] + \int \frac{(\mathbf{p}(\mathbf{r},t) - e\mathbf{A}(\mathbf{r},t))^2}{2m} n(\mathbf{r},t)d\mathbf{r} + \\ + e\int \phi(\mathbf{r},t)n(\mathbf{r},t)d\mathbf{r} + e\int V_{\text{back}}(\mathbf{r})n(\mathbf{r},t)d\mathbf{r}. \quad (1)$$

where $\mathbf{p}(\mathbf{r},t) = m\mathbf{v}(\mathbf{r},t) + e\mathbf{A}(\mathbf{r},t)$, is the canonical momentum of an electron in an electromagnetic field. The vector potential $\mathbf{A}(\mathbf{r},t)$ is associated with the electromagnetic field generated by the charge fluctuations. The retarded potential $\phi(\mathbf{r},t)$ is generated by the electron-electron interaction:

$$\phi(\mathbf{r},t) = \frac{e}{4\pi\varepsilon_0}\int \frac{n(\mathbf{r}',t_r)}{|\mathbf{r}-\mathbf{r}'|}\,d\mathbf{r}',$$

where $t_r = t - \frac{|\mathbf{r}-\mathbf{r}'|}{c}$. The potential $V_{\text{back}}(\mathbf{r})$ is an external confining potential for the electron gas. The functional $G[n(\mathbf{r},t)]$ is the internal energy of the electron gas, and it is given in general by the sum of the internal kinetic energy, the exchange energy, and the correlation energy of the electron system.

Supplementary Note 2

The equations of motion can be obtained by applying the general procedure of the Hamiltonian formulation of fluid mechanics [4, 5, 6] based on Poisson brackets (The procedure illustrated by Eguiluz in ref.[2] to calculate the equations of motion assumes that the canonical momentum $\mathbf{p}(\mathbf{r},t)$ is irrotational. The procedure reported here is more general, and it does not need any assumption on the properties of $\mathbf{p}(\mathbf{r},t)$). Following the argument by Lynch in ref. [4], in the Lagrangian formulation, the state of a fluid is fully described by the variables

$$\{\mathbf{r}(\mathbf{a},t),\mathbf{p}(\mathbf{a},t)\}, \quad (2)$$

where $\mathbf{a}$ are the Lagrangian coordinates of the fluid elements, $\mathbf{r}$ is the position of the fluid element labeled with $\mathbf{a}$, and $\mathbf{p}$ is the conjugate momentum of $\mathbf{r}$. For two given functionals of the Lagrangian

state of the fluid $F[\mathbf{r}(\mathbf{a}), \mathbf{p}(\mathbf{a})]$ and $G[\mathbf{r}(\mathbf{a}), \mathbf{p}(\mathbf{a})]$, the Poisson bracket reads

$$\{F, G\}_L = \int \Big\{ \frac{\delta F}{\delta \mathbf{r}(\mathbf{a})} \cdot \frac{\delta G}{\delta \mathbf{p}(\mathbf{a})} - \frac{\delta F}{\delta \mathbf{r}(\mathbf{a})} \cdot \frac{\delta G}{\delta \mathbf{p}(\mathbf{a})} \Big\} \, d\mathbf{a}. \tag{3}$$

In the Eulerian formulation, the state of the fluid is described by the Eulerian non-canonical variables (Temperature effects are not considered here, because the temperature of the system is fixed, $T = 0\,\mathrm{K}$. The processes studied here are isentropic).

$$\{n(\mathbf{r}, t), \mathbf{p}(\mathbf{r}, t)\}. \tag{4}$$

By applying the transformation from Lagrangian to Eulerian coordinates of the flow, it can be shown that, given two functionals $F(n, \mathbf{p})$ and $G(n, \mathbf{p})$ of the Eulerian state variables (4), the Poisson bracket (3) becomes [5, 7]

$$\{F, G\}_E = -\int \Big\{ \Big[\frac{\delta F}{\delta n} \nabla \cdot \frac{\delta G}{\delta \mathbf{p}} + \frac{\delta F}{\delta \mathbf{p}} \cdot \nabla \frac{\delta G}{\delta n} \Big] + \Big[\frac{\nabla \times \mathbf{p}}{n} \cdot \Big(\frac{\delta G}{\delta \mathbf{p}} \times \frac{\delta F}{\delta \mathbf{p}} \Big) \Big] \Big\} \, d\mathbf{r}, \tag{5}$$

that is called *hydrodynamic bracket* [5, 7], and it provides a Hamiltonian formulation in terms of the Eulerian variables (4).

The time evolution of the functional (observable) $F(\mathbf{p}, n)$ of a system described by the Hamiltonian functional H, can be calculated by means of the Poisson bracket (5)

$$\frac{\partial F}{\partial t} = \{F, H\}, \tag{6}$$

where H is the Hamiltonian (1). According to this approach, the evolution of the state variables of the system can be obtained by

$$\frac{\partial \mathbf{p}}{\partial t} = \{\mathbf{p}, H\}, \tag{7}$$

$$\frac{\partial n}{\partial t} = \{n, H\}. \tag{8}$$

For the electronic fluid described by the Hamiltonian (1), the time evolution of the state variables gives the equations of motion (see Supplementary Note 8)

$$\boxed{mn\Big(\frac{\partial \mathbf{v}}{\partial t} + \mathbf{v} \cdot \nabla \mathbf{v} \Big) = -n \nabla \frac{\delta G}{\delta n} + ne(\mathbf{E} + \mathbf{v} \times \mathbf{B})}, \tag{9}$$

$$\boxed{\frac{\partial n}{\partial t} = -\nabla \cdot (n\mathbf{v})} \tag{10}$$

where $\mathbf{E} \equiv -\nabla\phi - \frac{\partial \mathbf{A}}{\partial t}$ and $\mathbf{B} \equiv \nabla \times \mathbf{A}$ are the fields generated by the electron-density variations. Equation (9) is the Euler equation for the velocity field, and it is a force balance, where $mn\Big(\frac{\partial \mathbf{v}}{\partial t} + \mathbf{v} \cdot \nabla \mathbf{v} \Big)$ on the left-hand side represents the total force acting on the fluid element. The term $-n\nabla \frac{\delta G}{\delta n}$ represents a generalization of the conventional density-dependent pressure employed in fluid mechanics. Equation (10) is the continuity condition for the electron fluid.

Supplementary Note 3

The solution of the system of equations (9-10) can be approximated by means of perturbation theory. To this extent, the quantities in equation (9) and (10) can be expanded to first order as

$$\begin{aligned} n(\mathbf{r}, t) &= n_0(\mathbf{r}) + n_1(\mathbf{r}, t) \\ \Big(\frac{\delta G}{\delta n} \Big) &= \Big(\frac{\delta G}{\delta n} \Big)_0 + \Big(\frac{\delta G}{\delta n} \Big)_1 \\ \mathbf{v}(\mathbf{r}, t) &= \mathbf{v}_1(\mathbf{r}, t) \\ \mathbf{E}(\mathbf{r}, t) &= \mathbf{E}_0(\mathbf{r}) + \mathbf{E}_1(\mathbf{r}, t) \\ \mathbf{B}(\mathbf{r}, t) &= \mathbf{B}_1(\mathbf{r}, t), \end{aligned} \tag{11}$$

where the static density $n_0(\mathbf{r})$ is the equilibrium solution at $t = 0$, when no perturbation is present. The equilibrium velocity is $\mathbf{v}_0 = 0$, because no charges move at equilibrium. This also implies that the zero-order magnetic field $\mathbf{B}_0$ is identically zero.

The equilibrium condition is obtained when all the forces on the fluid element are in balance. This condition can be expressed by means of equation (9), that reads [in the following we will for simplicity suppress both the $(\mathbf{r}, t)$ and $(\mathbf{r})$ dependence]

$$-\nabla\Big(\frac{\delta G}{\delta n}\Big)_0 + e\mathbf{E}_0 - e\nabla V_{\text{back}} = 0, \tag{12}$$

where $\mathbf{E}_0$ is the electrostatic field generated by the charge density $n_0(\mathbf{r})$, that can be written as

$$\mathbf{E}_0 = -\nabla\phi_0,$$

where the static potential is given by

$$\phi_0 = \frac{e}{4\pi\varepsilon_0}\int \frac{n_0(\mathbf{r}')}{|\mathbf{r}-\mathbf{r}'|}\,d\mathbf{r}'.$$

This $\phi_0(\mathbf{r})$ satisfies the Poisson equation

$$\nabla^2\phi_0 = -\frac{en_0}{\varepsilon_0}. \tag{13}$$

It is important to notice that equation (12) can be written as

$$\nabla\Big[\Big(\frac{\delta G}{\delta n}\Big)_0 + e\phi_0 + eV_{\text{back}}\Big] = 0 \quad \forall\mathbf{r}, \tag{14}$$

because this means that the function in parentheses $[\cdot]$ is constant:

$$\boxed{\Big(\frac{\delta G}{\delta n}\Big)_0 + e(\phi_0 + V_{\text{back}}) = \mu} \tag{15}$$

where μ is constant. It can be shown that μ is the chemical potential of the electron system [8, 9].

The solution of equation (15) is the equilibrium electron density n_0. By inserting the expansions (11) into equation (9), one obtains the Euler equation for the first-order quantities,

$$m\frac{\partial\mathbf{v}_1}{\partial t} = -\nabla\Big(\frac{\delta G}{\delta n}\Big)_0 + e\mathbf{E}_0 - e\nabla V_{\text{back}} - \nabla\Big(\frac{\delta G}{\delta n}\Big)_1 + e\mathbf{E}_1.$$

By recalling the equilibrium condition (12), this equation becomes

$$m\frac{\partial\mathbf{v}_1}{\partial t} = -\nabla\Big(\frac{\delta G}{\delta n}\Big)_1 + e\mathbf{E}_1. \tag{16}$$

Analogously, the continuity equation (10) for the first-order quantities becomes

$$\nabla\cdot(n_0\mathbf{v}_1) = -\frac{\partial n_1}{\partial t}. \tag{17}$$

At this point, it is convenient to introduce the electric-charge density ρ_1, and the electric-current density $\mathbf{J}_1$ as

$$\rho_1 = en_1, \qquad \mathbf{J}_1 = en_0\mathbf{v}_1 \equiv \rho_0\mathbf{v}_1,$$

in terms of which equation (16) can be rewritten as

$$\boxed{\frac{\partial\mathbf{J}_1}{\partial t} = -\frac{\rho_0}{m}\nabla\Big(\frac{\delta G}{\delta n}\Big)_1 + \omega_p^2\varepsilon_0\mathbf{E}_1}, \tag{18}$$

where $\omega_p^2 = \frac{e^2 n_0}{m\varepsilon_0}$ is the spatially dependent plasma frequency of the electron gas. Also in terms of the new variables, equation (17) becomes

$$\boxed{\nabla\cdot\mathbf{J}_1 = -\frac{\partial\rho_1}{\partial t}}. \tag{19}$$

The electric field $\mathbf{E}_1$ satisfies Maxwell's wave equation:

$$\boxed{\nabla \times \nabla \times \mathbf{E}_1 + \frac{1}{c^2}\frac{\partial^2 \mathbf{E}_1}{\partial t^2} = -\mu_0 \frac{\partial \mathbf{J}_1}{\partial t}}. \tag{20}$$

The system of equations (18-19-20) allows one to solve for the first-order fields in our self-consistent hydrodynamic theory.

Supplementary Note 4

The SC-HDM implementation in COMSOL consists of two steps: the first step is the calculation of the equilibrium electron density, while the second step deals with the calculation of the first-order quantities.

The equilibrium electron density n_0 is a solution of the equation system (13-15), for the two unknown variables (n_0, ϕ_0). This system can be rewritten in terms of the single variable n_0, if we increase the differentiation order. In order to do that, we apply the $\nabla\cdot$ operator to both sides of equation (14)

$$\nabla^2\Big(\frac{\delta G}{\delta n}\Big)_0 + e\nabla^2\phi_0 + e\nabla^2 V_{\text{back}} = 0. \tag{21}$$

The potential V_{back} is generated by a uniform jellium background with density n^+, thus we can write

$$\nabla^2 V_{\text{back}} = \frac{en^+}{\varepsilon_0}. \tag{22}$$

At this point we can insert both equation (13) and equation (22) into equation (21), and obtain

$$\boxed{\nabla^2\Big(\frac{\delta G}{\delta n}\Big)_0 - \frac{e^2}{\varepsilon_0}n_0 + \frac{e^2}{\varepsilon_0}n^+ = 0}, \tag{23}$$

that is the equilibrium equation implemented in COMSOL.

The equations (18, 19, 20) can be rewritten in the frequency domain in terms of only one unknown quantity, the density ρ_1. Before doing that, we add a damping term to equation (18), with damping constant γ, that takes into account the electron-phonon interaction, dissipation due to the electron-hole continuum, impurity scattering, etc.:

$$\frac{\partial \mathbf{J}_1}{\partial t} = -\frac{\rho_0}{m}\nabla\Big(\frac{\delta G}{\delta n}\Big)_1 + \omega_p^2\varepsilon_0\mathbf{E}_1 - \gamma\mathbf{J}_1 \tag{24}$$

This equation can be written in the frequency domain as

$$\mathbf{J}_1 = \frac{1}{\gamma - i\omega}\Big[-\frac{\rho_0}{m}\nabla\Big(\frac{\delta G}{\delta n}\Big)_1 + \omega_p^2\varepsilon_0\mathbf{E}_1\Big]. \tag{25}$$

Likewise, equation (19) can be written in the frequency domain as

$$\nabla\cdot\mathbf{J}_1 = i\omega\rho_1. \tag{26}$$

At this point we can rewrite equation (25) by using the Gauss theorem for the electric field in the presence of a screening permittivity $\varepsilon_{\text{r}}(\omega)$ (as in the case in Ag due to of interband effects),

$$\nabla\cdot\mathbf{E}_1 = \frac{\rho_1}{\varepsilon_0\varepsilon_{\text{r}}(\omega)}. \tag{27}$$

If we apply the $\nabla\cdot$ operator to equation (25) and use equation (27), we obtain:

$$\boxed{i\omega\rho_1 = \frac{1}{\gamma - i\omega}\Big[-\nabla\cdot\frac{\rho_0}{m}\nabla\Big(\frac{\delta G}{\delta n}\Big)_1 + \varepsilon_0\mathbf{E}_1\cdot\nabla\omega_p^2 + \omega_p^2\frac{\rho_1}{\varepsilon_{\text{r}}(\omega)}\Big]}, \tag{28}$$

where we used the vector identity $\nabla \cdot (a\mathbf{B}) = \mathbf{B} \cdot \nabla a + a\, \nabla \cdot \mathbf{B}$. The Maxwell wave equation to be coupled with (28) is

$$\boxed{\nabla \times \nabla \times \mathbf{E}_1 = k_0^2 \varepsilon_{\rm r}(\omega)\mathbf{E}_1 + \frac{i\omega\mu_0}{\gamma - i\omega}\Big[- \frac{\rho_0}{m}\nabla\Big(\frac{\delta G}{\delta n}\Big)_1 + \omega_p^2 \varepsilon_0 \mathbf{E}_1\Big]}. \tag{29}$$

Equations (28 - 29) can readily be implemented in COMSOL, and they allow to solve for just one hydrodynamic quantity, ρ_1, instead of three quantities, the components of $\mathbf{J}_1$. This makes the COMSOL implementation more efficient.

Supplementary Note 5

In this section we will briefly discuss the computational efficiency of our COMSOL implementation of the SC-HDM, when applied to the cases examined in the main text. The 2D results presented in the main text are obtained on a personal computer with eight Intel 3.5Ghz processors and 32Gb of RAM. The only exceptions are the calculations of the resonance frequencies for the Bennett multipolar plasmon for $R > 10\,\text{nm}$ (Fig. 4 in the main text), that were calculated on a computer cluster equipped with nodes that can allocate up to 70GB of RAM. For the 3D calculations, we used the IC2 computer cluster facility at the Karlsruhe Institute of Technology, that allows to run simulations that require up to 512 GB of RAM on nodes equipped with four Octa-core Intel Xeon processors.

The first step of the SC-HDM is the calculation of the equilibrium density n_0 by means of the *nonlinear* equation (23). A high number of mesh elements (NME) is needed in order describe the density variations on the metal surface. In the case of a $R = 2\,\text{nm}$ nanowire, the NME is about $3 \cdot 10^5$, and the computational time (CT) is about 12 minutes. For a $R = 20\,\text{nm}$ nanorod, the NME is about $4 \cdot 10^5$ and the CT is about 20 minutes. These data hold for both Na and Ag nanowires. For the 3D nanospheres of $R = 1.5\,\text{nm}$, the NME is about $2 \cdot 10^5$ for the Na nanosphere, and $3 \cdot 10^5$ for the Ag nanosphere. A higher number of mesh elements is required for Ag, since the spillout layer extends on a smaller region compared to the Na case. The CT is about 6 hours for the Na nanosphere and 10 hours for the Ag one.

For the excited state calculation in 2D, the quantities (E_{1x}, E_{1y}, ρ_1) must be evaluated by means of the *linear* equation system (28 - 29), which requires a lower NME in order to reach convergence. We performed a convergence study for the observable $\sigma_{\rm abs}$ at the dipolar SPR as a function of the NME for both Na and Ag nanowires (Supplementary Figure 1). The relative error is given by $\delta = |\sigma_{\rm abs}^{\rm mesh} - \sigma_{\rm abs}^{\rm reg}|/\sigma_{\rm abs}^{\rm reg}$, where $\sigma_{\rm abs}^{\rm mesh}$ is the value of $\sigma_{\rm abs}$ at fixed NME and $\sigma_{\rm abs}^{\rm reg}$ is the value in the convergence regime.

The case of the Na nanowires with radii $R = 2\,\text{nm}$ and $R = 20\,\text{nm}$ is presented in Supplementary Figure 1a). For $R = 2\,\text{nm}$ the convergence is obtained for NME $\gtrapprox 6 \cdot 10^4$ elements, with a relative error $\delta < 0.07\%$ of the SPR frequency $\hbar\omega_{\rm res} = 4.017\,\text{eV}$. For $R = 20\,\text{nm}$ the convergence is reached for NME $\gtrapprox 18 \cdot 10^4$, with relative error $\delta < 0.02\%$ of the SPR frequency $\hbar\omega_{\rm res} = 3.9539\,\text{eV}$. The CT is about 1.5 minutes in the first case, and about 4 minutes in the second case.

The results of the convergence studies for the Ag nanowires with $R = 2\,\text{nm}$ and $R = 20\,\text{nm}$ are presented in Supplementary Figure 1b). For $R = 2\,\text{nm}$ the convergence is reached for NME $\gtrapprox 8 \cdot 10^4$ elements, with $\delta < 0.05\%$ of the SPR frequency $\hbar\omega_{\rm res} = 3.653\,\text{eV}$. For a $R = 20\,\text{nm}$ the convergence is obtained for NME $\gtrapprox 19 \cdot 10^4$, with $\delta < 0.02\%$ of the SPR frequency value $\hbar\omega_{\rm res} = 3.564\,\text{eV}$. The CT is comparable to the respective cases for Na nanowires.

The calculation of the resonance frequency for the "Bennett" multipolar resonances requires a higher NME respect to the dipolar SPR case. This is due to the fact that the charges have a "double layer" distribution about the surface edge, as we discussed in the main text. The NME is bigger than $35 \cdot 10^4$ for nanowires of radii $R > 10\,\text{nm}$, that is the maximum NME that our PC could handle.

Finally, for the excited-state calculation in 3D, the quantities $(E_{1x}, E_{1y}, E_{1z}, \rho_1)$ must be evaluated, but in this case we used the same NME employed for the n_0 calculation. The CT for each frequency for the Na nanosphere is about 1.5 hours, while it is about 2 hours for the Ag nanosphere. The RAM occupation is about 180 GB in the first case, while it is about 230 GB in the second case. Some strategies could be put in place in order to lower the computational complexity, but

no performance optimization study has been conducted at this stage of the 3D SC-HDM code development.

Supplementary Note 6

As we stated in the main text, we implemented our SC-HDM in COMSOL for practical reasons, since it offers a quite flexible implementation of the finite-element method and it is one of the increasingly used commercial codes in the field of plasmonics. However, other computational schemes can be adopted, and ad-hoc solvers could be developed. These solvers could be based, for example, on other discretization techniques, such as the finite-volume method (FVM), that is widely employed in fluid dynamics. This could be done by extending some of the routines of the well-known OpenFOAM computational toolbox, which is based on the FVM method. Another interesting alternative would be the discontinuous Galerkin method that combines appealing features of the FEM and the FVM. Finally, an ad-hoc computationally code could be advantageous, since COMSOL is a proprietary software, and it does not allow modifying and adapting the computational routines to the specific electrodynamics equations.

Supplementary Note 7

In this section we will benchmark the results obtained with the SC-HDM against those obtained with ab-initio methods. We start from the 2D case by comparing the absorption spectrum for a Na nanowire with radius $R = 2\,\mathrm{nm}$ obtained by means of the SC-HDM with the one calculated with the TD-DFT Octopus package in ref 10. Both results are presented in Supplementary Figure 2. It can be observed that the dipolar SPR peak for the TD-DFT case occurs at $\hbar\omega_{\mathrm{res}} = 4.09\,\mathrm{eV}$, while it occurs at $\hbar\omega_{\mathrm{res}} = 4.017\,\mathrm{eV}$ in the SC-HDM. The Bennett resonance is observed both in the SC-HDM and TD-DFT model, but it appears at $\hbar\omega_{\mathrm{res}} = 4.918\,\mathrm{eV}$ and $\hbar\omega_{\mathrm{res}} = 4.60\,\mathrm{eV}$ respectively. The linewidth obtained with the SC-HDM is narrower than for the TD-DFT calculations, one reason being (as discussed in the main text) the neglect of Landau damping in the SC-HDM. Apart from this, it is important to point out that both methods rely on different approximations, therefore a perfect agreement is neither reachable nor expected.

For the 3D calculations, we benchmarked our SC-HDM results for the sphere of radius $R = 1.5\,\mathrm{nm}$ against those obtained by Li et *et al.* in ref 11 by means of the Time-Dependent Local Density Approximation (TD-LDA). A direct comparison is not possible in this case, since Li *et al.* study the optical response of Na atomic clusters without employing the jellium model. The biggest cluster considered in their analysis is Na_{331}, which has an effective cluster radius $R_{\mathrm{C}} = 1.439\,\mathrm{nm}$. The absorption spectra obtained with both methods are shown in Supplementary Figure 3. It is possible to observe that the SPR dipolar resonance for the TD-LDA case is redshifted with respect to the one obtained with the SC-HDM. This is due to the fact that the radius of the Na_{331} cluster is smaller than the one of the SC-HDM sphere. Moreover, the resonance peaks are broadened in the TD-LDA case, and the Bennett resonance is strongly damped. This difference with the SC-HDM method can also be to a large part attributed to the neglection of Landau damping in our SC-HDM.

Supplementary Note 8

Here we will show how to derive equation (10) and (9) from the equations of motion for the density and its conjugate momentum, repectively. Both equations of motion are derived using the Poisson bracket (5), in combination with the Hamiltonian (1). The equation of motion (7) for the conjugate momentum $\mathbf{p}$ reads:

$$\frac{\partial p_i}{\partial t} = \{p_i, H\} = -\int \left\{ \left[\frac{\delta p_i}{\delta n} \nabla \cdot \frac{\delta H}{\delta \mathbf{p}} + \frac{\delta p_i}{\delta \mathbf{p}} \cdot \nabla \frac{\delta H}{\delta n} \right] + \left[\frac{\nabla \times \mathbf{p}}{n} \cdot \left(\frac{\delta H}{\delta \mathbf{p}} \times \frac{\delta p_i}{\delta \mathbf{p}} \right) \right] \right\} d\mathbf{r}', \tag{30}$$

where p_i indicates the i-th component of the vector $\mathbf{p}$. The functional associated with p_i is:

$$p_i(\mathbf{r}, t) = \int \mathbf{p}(\mathbf{r}, t) \cdot \mathbf{e}_i \delta(\mathbf{r} - \mathbf{r}')\, d\mathbf{r}', \tag{31}$$

where $\mathbf{e}_i$ is the unit vector of the i-th coordinate axis. The functional derivatives of $\mathbf{p}$ are then [4, 5]

$$\frac{\delta p_i}{\delta \mathbf{p}} = \mathbf{e}_i \delta(\mathbf{r} - \mathbf{r}'), \tag{32}$$

$$\frac{\delta p_i}{\delta n} = 0. \tag{33}$$

The functional derivatives of the Hamiltonian in equation (30) then become

$$\frac{\delta H}{\delta n} = \frac{(\mathbf{p} - e\mathbf{A})^2}{2m} + e\phi + \frac{\delta G}{\delta n}, \tag{34}$$

$$\frac{\delta H}{\delta \mathbf{p}} = n\frac{(\mathbf{p} - e\mathbf{A})}{m}, \tag{35}$$

which inserted into the equation of motion (30) gives

$$\frac{\partial p_i}{\partial t} = -\int \Big\{ \Big[\mathbf{e}_i \delta(\mathbf{r} - \mathbf{r}') \cdot \nabla \Big(\frac{(\mathbf{p} - e\mathbf{A})^2}{2m} + e\phi + \frac{\delta G}{\delta n} \Big) \Big] + \\ + \Big[\frac{\nabla \times \mathbf{p}}{n} \cdot \Big(n \frac{(\mathbf{p} - e\mathbf{A})}{m} \times \mathbf{e}_i \delta(\mathbf{r} - \mathbf{r}') \Big) \Big] \Big\} d\mathbf{r}'.$$

The spatial integral can be performed and yields

$$\frac{\partial p_i}{\partial t} = -\mathbf{e}_i \cdot \nabla \frac{\delta G}{\delta n} - \nabla \Big(\frac{(\mathbf{p} - e\mathbf{A})^2}{2m} + e\phi \Big) - \nabla \times \mathbf{p} \cdot \Big(\frac{(\mathbf{p} - e\mathbf{A})}{m} \times \mathbf{e}_i \Big). \tag{36}$$

The first term in equation (36) can be worked out in *Einstein notation* as

$$\nabla \Big(\frac{(\mathbf{p} - e\mathbf{A})^2}{2m} + e\phi \Big) = \partial_h \Big(\frac{(p_g - eA_g)^2}{2m} + e\phi \Big) \delta_{hi} = m v_g \partial_i v_g + e \partial_i \phi. \tag{37}$$

In the same way, the second term in equation (36) becomes

$$\nabla \times \mathbf{p} \cdot \Big(\frac{(\mathbf{p} - e\mathbf{A})}{m} \times \mathbf{e}_i \Big) = \varepsilon_{lmn} \partial_m p_n \varepsilon_{lgh} \frac{p_g - eA_g}{m} \delta_{hi} = \\ = \varepsilon_{lmn} \varepsilon_{lgi} \partial_m (m v_n + eA_n) v_g = \varepsilon_{lmn} \varepsilon_{lgi} \partial_m m v_n + \varepsilon_{lmn} \varepsilon_{lgi} e \partial_m A_n v_g. \tag{38}$$

This long equation can be simplified, using the mathematical identity

$$\varepsilon_{lmn} \varepsilon_{lgi} = [\delta_{mg} \delta_{ni} - \delta_{mi} \delta_{ng}],$$

into the more appealing form

$$\nabla \times \mathbf{p} \cdot \Big(\frac{(\mathbf{p} - e\mathbf{A})}{m} \times \mathbf{e}_i \Big) = m v_g \partial_g v_i - m v_g \partial_i v_g - e \varepsilon_{igl} v_g B_l, \tag{39}$$

where we also used the well-known relation between the magnetic field and the vector potential

$$\mathbf{B} = \nabla \times \mathbf{A} = \varepsilon_{lmn} \partial_m A_n.$$

By summing equations (37) and (38) we obtain on the right-hand side

$$\ldots = m v_g \partial_g v_i + e \partial_i \phi - e \varepsilon_{igl} v_g B_l.$$

Thus, equation (30) can be written as

$$m \frac{\partial v_i}{\partial t} + e \frac{\partial A_i}{\partial t} = -\partial_i \Big(\frac{\delta G}{\delta n} \Big) - m v_g \partial_g v_i - e \partial_i \phi + e \varepsilon_{igl} v_g B_l, \tag{40}$$

which in vectorial notation reads

$$m \Big(\frac{\partial \mathbf{v}}{\partial t} + \mathbf{v} \cdot \nabla \mathbf{v} \Big) = -\nabla \frac{\delta G}{\delta n} + e(\mathbf{E} + \mathbf{v} \times \mathbf{B}).$$

Hereby we showed how to obtain equation (9) from the equation of motion for the conjugate momentum.
In a similar fashion, we will now show how equation (10) can be obtained from the equation of motion for the density n,

$$\frac{\partial n}{\partial t} = \{n, H\} = -\int \left\{ \left[\frac{\delta n}{\delta n} \nabla \cdot \frac{\delta H}{\delta \mathbf{p}} + \frac{\delta n}{\delta \mathbf{p}} \cdot \nabla \frac{\delta H}{\delta n} \right] + \left[\frac{\nabla \times \mathbf{p}}{n} \cdot \left(\frac{\delta H}{\delta \mathbf{p}} \times \frac{\delta n}{\delta \mathbf{p}} \right) \right] \right\} d\mathbf{r}'. \tag{41}$$

Also in this case, n can be written as

$$n(\mathbf{r}, t) = \int n(\mathbf{r}, t) \delta(\mathbf{r} - \mathbf{r}')\, d\mathbf{r}',$$

and the functional derivatives in equation (41) become:

$$\frac{\delta n}{\delta n} = \delta(\mathbf{r} - \mathbf{r}'), \tag{42}$$

$$\frac{\delta n}{\delta \mathbf{p}} = 0. \tag{43}$$

By recalling equation (35), the equation of motion (41) turns into

$$\frac{\partial n}{\partial t} = -\int \left\{ \left[\frac{\delta n}{\delta n} \nabla \cdot \frac{\delta H}{\delta \mathbf{p}} \right] d\mathbf{r}' = -\nabla \cdot (n\mathbf{v}), \right.$$

which is indeed the continuity equation (10).

Supplementary Note 9

In the HW-HDM, the hydrodynamic model that is commonly used in nanoplasmonics, the uniform background ions with density n^+ are screened by an electron distribution of equal density $n_0(\mathbf{r}) = n^+$ inside the metal, and $n_0(\mathbf{r}) = 0$ in the free-space region that extends outside the metal. We want to show here that this simple form of $n_0(\mathbf{r})$ is a solution of equation (23), when the functional $G_{\mathrm{TF}}[n]$ is given by the Thomas-Fermi functional $T_{\mathrm{TF}}[n]$, that is the functional employed in the HW-HDM. We recall that the functional $T_{\mathrm{TF}}[n]$ is given by

$$T_{\mathrm{TF}}[n] = C_{\mathrm{TF}} n_0^{5/3}(\mathbf{r}),$$

with $C_{\mathrm{TF}} = \frac{3}{10}\frac{\hbar^2}{m}(3\pi^2)^{2/3}$.

Inside the metal, equation (23) reads

$$\frac{5}{3} C_{\mathrm{TF}} \nabla^2 n_0^{2/3}(\mathbf{r}) - e^2 \frac{n_0(\mathbf{r})}{\varepsilon_0} + e^2 \frac{n^+}{\varepsilon_0} = 0,$$

that is satisfied by the constant solution $n_0(\mathbf{r}) = n^+$.

Outside the metal domain, equation (23) reads

$$\frac{5}{3} C_{\mathrm{TF}} \nabla^2 n_0^{2/3}(\mathbf{r}) - e^2 \frac{n_0(\mathbf{r})}{\varepsilon_0} = 0, \tag{44}$$

because no ions are present in this region. It is then evident that equation (44) is satisfied by the vanishing constant density $n_0(\mathbf{r}) = 0$.

We have hereby shown that the step-function density distribution $n_0(\mathbf{r})$, that is chosen on the basis of physical arguments, satisfies equation (15), provided that the functional $G_{\mathrm{TF}}[n]$ is given by the Thomas-Fermi functional $T_{\mathrm{TF}}[n]$. For this reason, the HW-HDM complies with the same self-consistency requirement of Supplementary Note 3 that we also applied to our SC-HDM with spill-out.

Supplementary References

[1] F. Bloch, *Bremsvermögen von Atomen mit mehreren Elektronen*, Zeitschrift für Physik **81** (1933), 363-376.

[2] A. Eguiluz and J. J. Quinn, *Hydrodynamic model for surface plasmons in metals and degenerate semiconductors*, Phys. Rev. B **14**, 1347-1361 (1976).

[3] S. Lundqvist and N. H. March, *Theory of the inhomogeneous electron gas*, (Springer-Verlag New York, 1983).

[4] P. Lynch, *Hamiltonian methods for geophysical fluid dynamics: An introduction* (IMA, University of Minnesota, Preprint 1838, 2002).

[5] P. J. Morrison, *Hamiltonian description of the ideal fluid*, Rev. Mod. Phys. **70**, 467-521 (1998).

[6] P. J. Morrison, *Hamiltonian and action principle formulations of plasma physics*, Physics of Plasmas **12**, 058102 (2005).

[7] P. J. Morrison and J. M. Greene, *Noncanonical hamiltonian density formulation of hydrodynamics and ideal magnetohydrodynamics*, Phys. Rev. Lett. **45**, 790-794 (1980).

[8] R. M. Martin, *Electronic structure: Basic theory and practical methods*, (Cambridge University Press, 2008).

[9] E. Zaremba and H. C. Tso, *Thomas-Fermi-Dirac-von Weizsäcker hydrodynamics in parabolic wells*, Phys. Rev. B **49** , 8147-8162 (1994).

[10] Stella, L.; Zhang, P.; García-Vidal, F. J.; Rubio, A.; García-González, P. Performance of Nonlocal Optics When Applied to Plasmonic Nanostructures. *J. Phys. Chem. C* **117**, 8941-8949 (2013).

[11] Li, J.-H.; Hayashi, M.; Guo, G.-Y. Plasmonic excitations in quantum-sized sodium nanoparticles studied by time-dependent density functional calculations. *Phys. Rev. B* **88**, 155437 (2013).